Research Square

Preprints are preliminary reports that have not undergone peer review.
They should not be considered conclusive, used to inform clinical practice,
or referenced by the media as validated information.

Coronal compensation of pelvic obliquity in degenerative lumbar scoliosis: A classification based on pelvic obliquity orientation and global coronal balance

Xing Chen
First Affiliated Hospital of Wenzhou Medical University
Rongkun Xu
Qilu Hospital of Shandong University
Wenyang Fu
Qilu Hospital of Shandong University
Lianlei Wang
Qilu Hospital of Shandong University
Honglin Teng
First Affiliated Hospital of Wenzhou Medical University
Xinyu Liu
newyuliu@163.com
Qilu Hospital of Shandong University

Research Article

Keywords: Coronal compensation, Degenerative lumbar scoliosis, Deformity, Pelvic obliquity, Global coronal balance, Paraspinal muscle, Patient-reported outcomes

Posted Date: April 29th, 2026

DOI: https://doi.org/10.21203/rs.3.rs-9305101/v1

License: This work is licensed under a Creative Commons Attribution 4.0 International License. Read Full License

Additional Declarations: No competing interests reported.

Abstract

Background and objectives: Few studies have investigated the interaction between pelvic obliquity (PO) and coronal balance in degenerative lumbar scoliosis (DLS). This study investigated whether PO compensates for global coronal balance or regional scoliosis in DLS and compared radiographic and clinical outcomes between different PO orientations.

Methods: This study included 166 DLS patients. Coronal parameters included coronal balance distance (CBD), main Cobb angle (MC), fractional Cobb angle (FC), and PO. Patients were categorized as Type 1 (PO tilting toward the main curve) or Type 2 (PO tilting opposite the main curve). Based on CBD, patients were further classified as coronal balanced (Type A), coronal imbalance shifted toward the concavity (Type B), or coronal imbalance shifted toward the convexity (Type C). Evaluation of the PSM on magnetic resonance imaging were conducted preoperatively.Clinical included visual analogue scale (VAS), Oswestry Disability Index (ODI), and Scoliosis Research Society-22R (SRS-22R).

Results: The patients were divided into 67 with A1, 18 with A2, 28 with B1, 6 with B2, 24 with C1, and 11 with C2. Patients in Type 2 exhibited greater FC, vertebral rotation, and lateral listhesis at L4-5 and L5-S1, as well as more severe degeneration and asymmetrical degeneration of lumbosacral PSM. Additionally, type C2 exhibited the poorest VAS-back, SRS-pain and activity domains. In type 1, PO was significantly correlated with MC and MC-FC. In type 2, PO was significantly correlated with FC. No significant correlation was found between PO and CBD in either type.

Conclusion: In DLS patients, PO participates in compensating for local scoliotic curve rather than global coronal balance. Patients with PO oriented opposite the main curve demonstrated more severe three-dimensional deformity of the lower lumbar region and inferior pain and activity related outcomes, which may be associated with more severe and asymmetric degeneration of paraspinal muscles.

Introduction

Degenerative lumbar scoliosis (DLS) is an increasingly prevalent spinal disorder characterized by progressive three-dimensional deformity, which has been attributed to reduced health-related quality of life among the older population.[1-3] Restoring an ideal sagittal alignment following corrective surgery is a primary goal of spinal deformity correction surgeries for DLS patients given that such alignment is strongly correlated with patient-reported outcomes (PROMs).[4-6] Moreover, recent studies have increasingly highlighted the importance of comprehensively assessing coronal balance, which could also adversely impact patient satisfaction.[2,7-9]

The spinopelvic complex plays a critical role in maintaining global alignment. To maintain an upright posture, patients need to engage compensatory mechanisms involving the spine and pelvis (i.e., pelvic retroversion, thoracic hyperextension, and hip flexion)[2,5,6]. In recent years, the involvement of paraspinal muscles (PSM) in the onset and progression of DLS has been widely discussed[10-13]. Patients with diminished PSM muscularity typically have lower compensatory capacity and are more likely to develop coronal imbalance[12]. Conversely, patients presenting with strong muscularity could maintain coronal balance postoperatively[10]. The anatomy and function of PSM influence both the spine and pelvis, playing a crucial role in preserving spinopelvic stability and maintaining postural balance[13-15].

As spinal deformity surpasses the compensatory capacity of the available PSM muscularity, pelvic compensation mechanisms become increasingly engaged[14,15]. Pelvic obliquity (PO) is a common compensation for a scoliotic curve in DLS[16]. Adult spinal deformity patients at the highest risk of postoperative coronal imbalance showed higher preoperative PO[17-19]. However, it remains debated whether PO primarily compensates for scoliosis deformity or global coronal balance.[16,18,20]

It is plausible to hypothesize that different pelvic coronal orientations reflect distinct compensatory mechanisms. In the present study, we hypothesized that PO develops as a compensatory phenomenon in response to regional scoliotic deformity. We also analyzed the radiographic and clinical outcomes of different pelvic obliquity orientations.

Methods

This study was approved by the Ethical Board Review of our institution. The present study retrospectively collected DLS patients that attended our hospital from January 2018 to October 2024.

Inclusion criteria were those aged between 50 to 80 years old, medical records containing anteroposterior and lateral full spine X-ray radiographs and magnetic resonance imaging (MRI) of the lumbar spine, coronal Cobb angle greater than 20°, and PO greater than 1 degree. Exclusion criteria were history of scoliosis in childhood or adolescence, history of prior spine surgery, hip or knee arthroplasty, systemic diseases that can affect spinal alignment (such as ankylosing spondylitis, Parkinson disease, etc.), an absolute discrepancy of leg length >20mm, and PO less than 1 degree. Basic demographics including age, sex, body mass index, smoking status, and medical comorbidities were extracted from the patients' electronic medical records.

Radiographic and clinical data collection

A full-spine anteroposterior and lateral radiograph was obtained for patients enrolled in this study. As shown in Figure 1, sagittal parameters included sagittal vertical axis (SVA), thoracic kyphosis (TK), lumbar lordosis (LL), lumbosacral lordotic angle (LSLA), pelvic incidence (PI), pelvic tilt (PT), and sacral slope (SS). Coronal parameters included: coronal balance distance (CBD), Cobb angle of main curve (MC), Cobb angle of lumbosacral fractional curve (FC) and pelvic obliquity (PO). Location of upper end vertebrae (UEV), lower end vertebrae (LEV) and apex vertebrae (AV), vertebras in the major curve, vertebral rotatory subluxation (VRS), vertebral lateral translation of L3-4 and L4-5, rotation of apex vertebrae, L4 and L5 vertebras (Nash-Moe index) were recorded[21,22].Vertebrae from L1 to L5 were assigned numbers ranging from 1 to 5 to facilitate data analysis for apical vertebrae. The degree of intervertebral disc degeneration was assessed according to the modified Pfirrmann grading system[23]. Patient-reported outcomes including visual analog scale for back pain (VAS-back), visual analog scale for leg pain (VAS-leg), Oswestry Disability Index (ODI), and Scoliosis Research Society-22 (SRS-22) scores were collected.

Pelvic obliquity type was represented by the orientation of pelvic obliquity relative to the main curve: Type 1, indicated that PO coronally tilt towards the convex side of the main curve; Type 2, indicated that PO coronally tilt towards the concave side of the main curve.

Morphological evaluation of the paraspinal muscle

The lumbar MRI images were acquired on the routine 1.5-T MR Scanner (AERA, Siemens). We obtained five T2-weighted axial images for the intervertebral disc levels from the preoperative MRI. Paraspinal muscles (PSM) were assessed from the center slice of each of the five images from L1 to L5. Bilateral cross-sectional area (CSA) of PSM was measured by outlining the fascial boundary at targeted slices using ImageJ software (Figure 1C). Fat infiltration rate (FI%) of the PSM was obtained by threshold technique as previously reported. To facilitate comparison of the PSM morphology and degeneration between concave and convex sides, the asymmetric degree in PSM CSA (aCSA) and PSM FI% (aFI) was calculated as follows: aCSA = CSA_{convex}- $CSA_{concave}$; aFI = $FI\%_{concave}$-$FI\%_{convex}$.

Statistical Analysis

Statistical analysis was performed using SPSS computer software (version 24; SPSS, Chicago, IL). Between-group comparisons of continuous variables and categorical variables were performed using independent t test. One-way ANOVA and Bonferroni Post-hoc test were used for inter-group comparisons. Categorical variables were compared using the X2 test or Fisher's exact test. Pearson's correlation test was used to analyze the correlation between different parameters. Statistical significance was set at $p < 0.05$.

Results

Group Description

In patients with PO less than 1 degree, the intraclass correlation coefficients (ICCs) for intra-rater and inter-rater were 0.541 and 0.605, respectively, indicating poor reliability. However, when the PO exceeded 1 degree, the ICCs for intra-rater and inter-rater increased to 0.811 and 0.805, respectively, indicating good reliability. Therefore, to minimize bias resulting from measurement error, the present study excluded patients with a PO less than 1 degree. Finally, a total of 166 patients were enrolled in the analysis, including 139 females and 27 males, with an average age of 61.87 years. According to Nanjing coronal classifications as previously defined by Qiu et al.[24], 97 patients were classified as type A, 34 as type B, and 35 as type C. According to PO orientation, 132 patients were categorized into Type 1, and 34 patients were categorized into Type 2. The patient distribution after combining Nanjing coronal classification and PO is shown in Figure 2. The baseline characteristics of the patients are summarized in Table 1.

Curve characteristics and Radiographic measures

As shown in Figure 2, the upper end vertebrae are located more cephalad in Type 1 patients, whereas the upper end vertebrae are located more caudal in Type 2 patients. Similar trend was found in apical vertebrae distribution (2.39 ± 0.48 vs. 3.10 ± 0.94, p=0.027). The number of vertebrae in the main curve was nonsignificantly larger in Type 1 than in Type 2 (4.43 ± 1.01 vs. 3.86 ± 0.87, p=0.073). No significant difference was found in the modified Pfirrmann grade between the two types. Although no significant differences in segmental VRS were observed between the two types, Type 2 patients demonstrated significantly greater lateral listhesis at L3–4 and L4–5 levels compared with Type 1 patients (L3/4: 3.54 ± 1.18 vs. 5.39 ± 1.95, p= 0.036; L4/5: 3.07 ± 1.20 vs. 5.56 ± 2.14, p=0.015). With respect to coronal parameters, Type 2 patients showed smaller MC Cobb (29.84 ± 11.71° vs. 38.80 ± 17.82°, p=0.037), greater FC Cobb (23.21 ± 7.22° vs. 14.65 ± 3.2°, p=0.008), and smaller MC-FC (6.95 ± 3.31° vs. 24.07 ± 11.58°, p<0.001) than Type 1 patients. With respect to sagittal measurements, Type 2 showed lower LSLA than Type 1 (23.66 ± 12.08° vs. 28.15 ± 12.54°, p=0.036), while the other variables were comparable

between the 2 types. In comparison of vertebral rotation, the apex rotation showed no difference among two types (2.51 ± 0.69 vs. 2.72 ± 0.80, p=0.431), while the rotation of L4 and L5 was significantly greater in Type 2 (1.71 ± 0.54 vs. 2.43 ± 0.61; 1.55 ± 0.51 vs. 2.19 ± 0.56, p= 0.026; 0.045, respectively).

Comparison of PSM morphology between subtypes

No significant differences in FI% and CSA were found at upper lumbar regions (L1-L3). On the contrary, patients in Type 2 exhibited significantly more severe FI% of paraspinal extensor muscles at lumbosacral regions.

In comparison of L4-5 and L5-S1 PSM parameters, the mean FI% of PSM was significantly higher on the concave side compared to the convex side, and patients with Nanjing Type B and C exhibited more severe fat infiltration than those in Type A on both concave and convex sides, while no significant differences were observed between Type B and Type C (Table 3). No significant differences were found between Type 1 and Type 2 with regard to CSA. In the FI% assessment, patients in Type 2 demonstrated more severe PSM fat infiltration than those in Type 1 on both the concave and convex sides. Specifically, patients in the C2 group showed the most severe PSM degeneration especially on the concave sides, manifesting as average fat infiltration rates of 55.8 ± 14.5 at L4-5 level and 61.5 ± 21.6 at L5-S1 level.

Regarding the asymmetry in PSM morphology between the concave and convex sides in lumbosacral region PSM, the aFI was significantly higher in Type 2, and patients in the C2 group exhibited the most prominent asymmetric PSM degeneration (L4-5: 16.4 ± 3.9; L5-S1: 15.1 ± 6.3). No significant differences were observed in the aCSA among the groups (p>0.05).

Relationships between coronal parameters and lumbosacral region PSM

Correlation analysis among coronal parameters (Table 4): In Type 1, PO was significantly correlated with MC (r=0.467, p<0.01) and MC-FC (r=0.501, p<0.01), and FC was significantly correlated with MC (r=0.698, p<0.01). In type 2, both PO and MC were significantly correlated with FC (r=0.390, p<0.01; r=0.371, p<0.05).

Correlation analysis between coronal parameters and lumbosacral region PSM: In Type 1, PO was significantly correlated with CC-FI% (r=0.496, p<0.01), and MC was significantly correlated with aFI and CC-FI% (r=0.417, p<0.01; r=0.545, p<0.01), respectively. In Type 2, there was a correlation between aFI and PO (r=0.358, p<0.05), as well as FC (r=0.305, p<0.05), while none of the coronal parameters showed correlation with FI%. Besides, neither coronal parameters nor PSM parameters showed correlation with CBD in Types 1 and 2.

Comparison of PROMs

The C2 group showed the worst VAS-back pain scores. No significant differences in any SRS-22r domains were observed at baseline when comparing the Nanjing A and B types, while the pain domain in C2 group were significantly worse than those in C1 group, and C2 group showed the lowest scores in the pain domain across all subgroups. Moreover, compared with group C1, group C2 had significantly worse SRS-22 activity (2.2 ± 0.5 vs. 2.5 ± 0.6, p=0.031).

Discussion

Degenerative lumbar scoliosis is a complex disorder that impairs quality of life in the elderly population[5,10,25]. The human musculoskeletal system is inherently symmetrical, with the spine serving as the central axis and the muscles, bones, and forces distributed symmetrically. As described as “pelvic vertebra” in scoliosis, the pelvis is regarded as the distal component in the function and structure of the spine[26]. The cervical, thoracic, lumbar segments, and the pelvis are considered as 4 components of vertebral rotation in scoliosis, and once one segment becomes unstable, the other segments simultaneously compensate to maintain global balance[5,25,27,28].

Pelvic obliquity is a common compensatory phenomenon in coronal plane for a scoliotic curve[5,16,18,29]. PO is frequently observed in patients with adolescent idiopathic scoliosis (AIS), which compensates for shoulder balance or global coronal alignment in different conditions[29]. The current understanding of the significance of pelvic obliquity in DLS has been mainly derived from the AIS literature. To date, it remains debated whether PO primarily compensates for regional scoliotic curve or global coronal alignment, and there has been a paucity of studies about the underlying mechanism of the interaction of pelvis and spine in coronal plane in DLS patients[16,18,20]. In the present study, the mean PO was 2.4°, indicating a high prevalence of coronal pelvic compensation. Moreover, two distinct PO types were identified, each demonstrating unique radiographic and PSM characteristics. We observed several interesting points and summarize the observed results in Figure 3: (1) The distributions of AV and UEV in Type 1 was more cephalad compared to Type 2, and the number of vertebra included in the main curve was slightly greater in Type 1 patients. (2) Patients in Type 2 exhibited smaller MC, MC-FC and LSLA, but greater FC than Type 1. Besides, vertebral rotation and lateral translation of L4 and L5 vertebrae were significantly greater in Type 2, indicating that the lumbosacral curve is not merely a scoliotic curve in the coronal plane but constitutes a more severe three-dimensional deformity. (3) In Type 1, PO was correlated to MC and MC-FC, while no correlation was observed between PO and MC or PO and MC-FC in Type 2. On the contrary, PO was correlated to FC in Type 2, which was absent in Type 1. Additionally, it is worth noting that the correlation between lumbosacral region PSM and coronal parameters also differs between Type 1 and Type 2. In Type 1, PO and MC correlated with CC-FI%, while no correlation was determined between coronal parameters and aFI. On the contrary, in Type 2, there was a correlation between aFI and PO, as well as FC. (4) Patients in Type 2 exhibited more severe lumbosacral PSM fat infiltration and aFI of PSM compared to Type 1, especially those in C2 group. (5) Patients in C2 group had the worst VAS-back pain, SRS-22 pain and activity domains. In these individuals, the fatigue or spasms in the low back PSM may be the leading cause of pain exacerbations. Additionally, discomfort is probably the main cause of mobility limits, coupling with the diminished ability to maintain a balanced body posture in activity due to severe asymmetric PSM degeneration.

Taken together, these differences indicated distinct intrinsic synergistic interactions in two types, in which the degeneration of lumbosacral region PSM play a pivotal role. The spine and pelvis adapt to a configuration that is stabilized by the available paraspinal muscle muscularity, and the compensation recruitment of the pelvis increased since the severity of the spinal deformity surpassed the compensatory capacity of the paraspinal muscles[10-12,14]. In type 1 patients, the available PSM can function as an effective compensatory mechanism in synergy with PO to compensate for MC. However, patients in type 2 experienced further deterioration of lumbosacral PSM, and the compensatory capability of the PSM diminished. As a result, the severe deterioration and prominent asymmetric degeneration of lumbosacral PSM directly leads to exacerbation of FC and PO. Differing from previous reports which have confirmed significant positive correlations between PSM degeneration and Cobb angle, we found no correlation between MC and PSM parameters in Type 2. Moreover,

the cobb angle in type 1 is significantly larger than that in type 2, while the lumbosacral region PSM degeneration in type 2 is, paradoxically, more severe than in type 1. This raises the possibility that other factors such as upper region PSM and core muscles may occur simultaneously, which needs further configuration in a larger cohort[12,30,31]. Nevertheless, comparisons between the patients with Type 1 and Type 2 revealed no significant difference in CBD, and no correlation was found between PO and CBD in either type.

Limitations

The present study has some limitations. First, the primary limitation is its cross-sectional design, and the sample sizes were relatively small after being divided into 6 subgroups, which might result in bias and precludes confirmation of causality. Second, the analysis of PSM is mainly focused to the cranial levels, which protect against and distribute stress on the spine, and is more affected by FI which is a surrogate marker for loss of muscular strength. Lastly, compensatory mechanisms could also be influenced by hip muscle and lower-limb conditions, which were not addressed in the present study. However, patients with leg length discrepancy, osteoarthritis, and a history of joint replacement were excluded to minimize the confounding effects of lower-limb pathology.

Conclusion

PO appears to represent a compensatory mechanism for regional scoliotic deformity rather than for global coronal balance in DLS. Specifically, patients with PO oriented opposite to the main curve demonstrated more severe three-dimensional deformity in lumbosacral region and more severe degeneration of lumbosacral PSM. Moreover, patients in the C2 type demonstrated the most severe PSM degeneration and asymmetrical degeneration, as well as the worst pain and disability related outcomes.

References

1. Yilgor C, Sogunmez N, Boissiere L, et al. Global Alignment and Proportion (GAP) Score: Development and Validation of a New Method of Analyzing Spinopelvic Alignment to Predict Mechanical Complications After Adult Spinal Deformity Surgery. *J Bone Joint Surg Am*. Oct 4 2017;99(19):1661-1672. doi:10.2106/JBJS.16.01594
2. Kwon O, Lee S, Park SM, Yeom JS, Kim HJ. A Complement Type to SRS-Schwab Adult Spinal Deformity Classification: The Failure of Pelvic Compensation. *Spine (Phila Pa 1976)*. Sep 15 2022;47(18):1295-1302. doi:10.1097/BRS.0000000000004404
3. Lee CH, Chung CK, Jang JS, et al. Effectiveness of deformity-correction surgery for primary degenerative sagittal imbalance: a meta-analysis. *J Neurosurg Spine*. Nov 2017;27(5):540-551. doi:10.3171/2017.3.SPINE161134
4. Hagglund G. Association between pelvic obliquity and scoliosis, hip displacement and asymmetric hip abduction in children with cerebral palsy: a cross-sectional registry study. *BMC Musculoskelet Disord*. Jul 14 2020;21(1):464. doi:10.1186/s12891-020-03484-y
5. Le Huec JC, Thompson W, Mohsinaly Y, Barrey C, Faundez A. Sagittal balance of the spine. *Eur Spine J*. Sep 2019;28(9):1889-1905. doi:10.1007/s00586-019-06083-1

6. Wang D, Wang W, Wang Y, et al. Identification and impact of failure of pelvic compensation in patients with adult spinal deformity. *Spine J*. Nov 2024;24(11):2124-2134. doi:10.1016/j.spinee.2024.06.011
7. Lu S, Zhu W, Diwan AD, et al. Global Coronal Malalignment in Degenerative Lumbar Scoliosis and Priority-Matching Correction Technique to Prevent Postoperative Coronal Decompensation. *Global Spine J*. May 22 2023:21925682231178202. doi:10.1177/21925682231178202
8. Glassman SD, Berven S, Bridwell K, Horton W, Dimar JR. Correlation of radiographic parameters and clinical symptoms in adult scoliosis. *Spine (Phila Pa 1976)*. Mar 15 2005;30(6):682-8. doi:10.1097/01.brs.0000155425.04536.f7
9. Ramieri A, Miscusi M, Domenicucci M, Raco A, Costanzo G. Surgical management of coronal and sagittal imbalance of the spine without PSO: a multicentric cohort study on compensated adult degenerative deformities. *Eur Spine J*. Oct 2017;26(Suppl 4):442-449. doi:10.1007/s00586-017-5042-6
10. Chen X, Xu R, Yuan S, et al. The Role of Paraspinal Muscle in Postoperative Coronal Balance Transition in Degenerative Lumbar Scoliosis: A 2-year Follow-up Study. *Spine (Phila Pa 1976)*. Aug 27 2024;doi:10.1097/BRS.0000000000005132
11. Shang Z, Chang H, Xu J, Ding W, Wang H, Zhang D. Characteristic of Paraspinal Muscle Change in Coronal Sub-type of Degenerative Lumbar Scoliosis and its Potential Clinical Significance. *Orthop Surg*. Nov 2024;16(11):2722-2731. doi:10.1111/os.14185
12. Kiram A, Hu Z, Man GC, et al. The role of paraspinal muscle degeneration in coronal imbalance in patients with degenerative scoliosis. *Quant Imaging Med Surg*. Nov 2022;12(11):5101-5113. doi:10.21037/qims-22-222
13. Yagi M, Hosogane N, Watanabe K, Asazuma T, Matsumoto M, Keio Spine Research G. The paravertebral muscle and psoas for the maintenance of global spinal alignment in patient with degenerative lumbar scoliosis. *Spine J*. Apr 2016;16(4):451-8. doi:10.1016/j.spinee.2015.07.001
14. Yamato Y, Nojima O, Banno T, et al. Measuring Muscle Activity in the Trunk, Pelvis, and Lower Limb Which Are Used to Maintain Standing Posture in Patients With Adult Spinal Deformity, With Focus on Muscles that Contract in the Compensatory Status. *Global Spine J*. Oct 2023;13(8):2245-2254. doi:10.1177/21925682221079257
15. Bae J, Sathe A, Lee SM, Theologis AA, Deviren V, Lee SH. Correlation of Paraspinal Muscle Mass With Decompensation of Sagittal Adult Spinal Deformity After Setting of Fatigue Post 10-Minute Walk. *Neurospine*. Sep 2021;18(3):495-503. doi:10.14245/ns.2142510.255
16. Radcliff KE, Orozco F, Molby N, et al. Is pelvic obliquity related to degenerative scoliosis? *Orthop Surg*. Aug 2013;5(3):171-6. doi:10.1111/os.12055
17. Zuckerman SL, Lai CS, Shen Y, et al. Incidence and risk factors of iatrogenic coronal malalignment after adult spinal deformity surgery: a single-center experience. *J Neurosurg Spine*. Oct 22 2021:1-10. doi:10.3171/2021.6.SPINE21575
18. Zuckerman SL, Lai CS, Shen Y, et al. Understanding the role of pelvic obliquity and leg length discrepancy in adult spinal deformity patients with coronal malalignment: unlocking the black box. *J Neurosurg Spine*. Jan 14 2022:1-9. doi:10.3171/2021.10.SPINE21800
19. Lee NJ, Fields M, Hassan FM, et al. Predicting postoperative coronal alignment for adult spinal deformity: do lower-extremity factors matter? *J Neurosurg Spine*. Aug 1 2023;39(2):175-186. doi:10.3171/2023.3.SPINE221364

20. Zhang Z, Liu T, Wang Y, Wang Z, Zheng G. Factors Related to Preoperative Coronal Malalignment in Degenerative Lumbar Scoliosis: An Analysis on Coronal Parameters. *Orthop Surg*. Aug 2022;14(8):1846-1852. doi:10.1111/os.13379
21. Bao H, Zhu F, Liu Z, et al. Vertebral rotatory subluxation in degenerative scoliosis: facet joint tropism is related. *Spine (Phila Pa 1976)*. Dec 15 2014;39(26 Spec No.):B45-51. doi:10.1097/BRS.0000000000000494
22. Ploumis A, Transfeldt EE, Gilbert TJ, Jr., Mehbod AA, Dykes DC, Perra JE. Degenerative lumbar scoliosis: radiographic correlation of lateral rotatory olisthesis with neural canal dimensions. *Spine (Phila Pa 1976)*. Sep 15 2006;31(20):2353-8. doi:10.1097/01.brs.0000240206.00747.cb
23. Griffith JF, Wang YX, Antonio GE, et al. Modified Pfirrmann grading system for lumbar intervertebral disc degeneration. *Spine (Phila Pa 1976)*. Nov 15 2007;32(24):E708-12. doi:10.1097/BRS.0b013e31815a59a0
24. Bao H, Yan P, Qiu Y, Liu Z, Zhu F. Coronal imbalance in degenerative lumbar scoliosis: Prevalence and influence on surgical decision-making for spinal osteotomy. *Bone Joint J*. Sep 2016;98-B(9):1227-33. doi:10.1302/0301-620X.98B9.37273
25. Han SM, Yang C, Wen JX, et al. Morphology and deformity of the shoulder and pelvis in the entire spine radiographs of adolescent idiopathic scoliosis. *Quant Imaging Med Surg*. May 1 2023;13(5):3266-3278. doi:10.21037/qims-22-656
26. Qiu XS, Wang ZW, Qiu Y, et al. Preoperative pelvic axial rotation: a possible predictor for postoperative coronal decompensation in thoracolumbar/lumbar adolescent idiopathic scoliosis. *Eur Spine J*. Jun 2013;22(6):1264-72. doi:10.1007/s00586-013-2695-7
27. Ilharreborde B, Dubousset J, Le Huec JC. Use of EOS imaging for the assessment of scoliosis deformities: application to postoperative 3D quantitative analysis of the trunk. *Eur Spine J*. Jul 2014;23 Suppl 4:S397-405. doi:10.1007/s00586-014-3334-7
28. Ferrero E, Vira S, Ames CP, et al. Analysis of an unexplored group of sagittal deformity patients: low pelvic tilt despite positive sagittal malalignment. *Eur Spine J*. Nov 2016;25(11):3568-3576. doi:10.1007/s00586-015-4048-1
29. Banno T, Yamato Y, Hasegawa T, et al. Impact of pelvic obliquity on coronal alignment in patients with adolescent idiopathic scoliosis. *Spine Deform*. Dec 2020;8(6):1269-1278. doi:10.1007/s43390-020-00145-x
30. Lee JM, Lee DH, Chung NS, et al. Hip, Abdomen, and Paraspinal Muscle Morphologies and Their Correlation with Pain and Disability in Degenerative Lumbar Scoliosis Patients. *Spine (Phila Pa 1976)*. Apr 16 2025;doi:10.1097/BRS.0000000000005362
31. Lavu MS, Hecht CJ, 2nd, Kaelber DC, Grammatopoulos G, Homma Y, Kamath AF. Spine-Abductor Syndrome: Novel Associations Between Lumbar Spine Disease and Hip Gluteal Muscle Pathology. *J Bone Joint Surg Am*. Mar 5 2025;107(5):496-503. doi:10.2106/JBJS.24.00012

Tables

Table 1. Demographic information of total patient cohort and among the groups

Variable	Entire Cohort (n=166)	Type 1 (n=132)	Type 2 (n=34)
Age, y	61.87±9.13	62.04±9.26	61.32±8.85
Sex (M/F)	27/139	22/110	5/29
BMI, kg/m^2	23.91±3.76	23.80±3.68	24.01±4.02
History of smoking	13(7.8%)	10(7.6%)	3(8.8%)
Duration of symptoms, m	92.4±80.7	92.6±82.1	90.9±76.6
L1-L4 average T score	-1.4±1.5	-1.5±1.4	-1.4±1.6
Osteoporosis	75(45.2%)	60(45.5%)	15(44.1%)
Menopause	130(78.3%)	104(78.8%)	26(76.5%)
Hypertension	73(44.0%)	59(44.7%)	14(41.2%)
Diabetes mellitus	38(22.9%)	30(22.7%)	8(23.5%)
Coronary artery disease	12(7.2%)	9(6.8%)	3(8.8%)

BMI, body mass index

Values represented as mean ± standard deviation

Numbers represented as n (percent%)

Table 2 is not available with this version.

Table 3. Comparison of the L4-L5 and L5-S1 Paraspinal Muscle Characteristics across the six subgroups

	A1	A2	B1	B2	C1	C2	P-value	Post-hoc test
L4-L5								
CC-CSA	18.2±3.5	17.9±3.9	17.6±5.3	16.1±6.5	18.0±4.7	17.5±4.9	0.352	-
CV-CSA	17.4±3.3	16.4±3.6	15.5±4.1	14.9±7.4	15.3±4.6	15.1±5.2	0.544	-
aCSA	0.9±2.3	1.4±1.7	2.0±2.4	2.3±3.2	2.6±2.6	2.5±3.0	0.670	-
CC-FI%	33.5±8.7	38.7±9.0	39.3±12.1	47.9±15.5	40.9±10.8	55.8±14.5	0.085	A1 vs. A2*; B1 vs. B2***; C1 vs. C2***
CV-FI%	28.6±7.4	31.6±8.2	32.5±11.6	37.1±14.6	31.7±9.5	40.2±13.4	0.318	C1 vs. C2*
aFI	5.0±3.4	7.3±4.9	7.0±5.1	11.2±6.0	9.3±4.4	16.4±3.9	0.196	B1 vs. B2**; C1 vs. C2***
L5-S1								
CC-CSA	17.1±3.7	16.4±3.4	17.0±4.7	16.5±5.6	16.7±5.0	17.9±5.4	0.547	-
CV-CSA	16.6±4.0	15.4±3.7	15.7±5.6	15.2±6.9	15.0±5.3	15.7±5.5	0.416	-
aCSA	0.5±0.8	1.1±1.4	1.3±1.9	1.4±2.1	1.8±2.0	2.1±2.2	0.489	-
CC-FI%	39.1±13.5	46.2±14.9	44.9±15.4	53.4±24.1	48.7±18.5	61.5±21.6	0.046	A1 vs. A2*; B1 vs. B2**; C1 vs. C2***
CV-FI%	31.7±14.7	35.1±13.5	35.0±12.8	39.5±16.0	38.0±14.6	45.9±15.2	0.233	C1 vs. C2*
aFI	7.5±3.6	11.9±4.0	10.2±4.9	14.2±5.1	11.0±5.4	15.1±6.3	0.095	A1 vs. A2**; B1 vs. B2**; C1 vs. C2**

CC-CSA, concave cross-sectional area; CV-CSA, convex cross-sectional area; aCSA, asymmetry of cross-sectional area; CC-FI%, concave fat infiltration rate; CV-FI%, convex fat infiltration rate; aFI, asymmetry of cross-sectional area

*** indicates p value <0.01; ** indicates p value <0.01; * indicates p value <0.05.

Table 4. Pearson correlation and r value of the coronal parameters and L4-S1 PSM parameters among two types

Type 1								
	MC	FC	MC-FC	PO	CBD	aFI	CC-FI%	CV-FI%
MC	×	0.587**	0.698**	0.467**	0.043	0.417**	0.582**	0.545**
FC	×	×	-0.590**	0.292*	0.103	0.127	0.066	0.074
MC-FC	×	×	×	0.501**	-0.114	0.235*	0.117*	0.098
PO	×	×	×	×	0.181	0.086	0.496**	0.410*
CBD	×	×	×	×	×	-0.039	0.233	0.159
Type 2								
	MC	FC	MC-FC	PO	CBD	aFI	CC-FI%	CV-FI%
MC	×	0.371*	0.643**	0.174	0.115	0.140	0.212	0.165
FC	×	×	-0.701**	0.390**	0.267	0.305*	0.128	0.173
MC-FC	×	×	×	0.192	0.096	-0.122	-0.014	-0.035
PO	×	×	×	×	0.135	0.358*	0.205	-0.089
CBD	×	×	×	×	×	0.052	0.133	0.098

MC, main Cobb; FC, fractional Cobb; MC-FC, main Cobb minus fractional Cobb; PO, pelvic obliquity; CBD, coronal balance distance.

* Indicates $p < 0.05$(two-tailed); ** Indicates $p < 0.01$(two-tailed);

Table 5. Comparison of preoperative clinical outcomes across the six groups

Variables	A1	A2	B1	B2	C1	C2	P value	Post hoc test
VAS-back	6.3±1.9	6.3±1.8	6.3±1.8	6.5±2.5	6.3±2.2	6.7±2.1	0.186	C1 vs. C2*
VAS-leg	6.1±1.8	6.2±1.9	6.2±1.9	5.9±2.7	6.1±2.1	6.2±2.0	0.473	-
ODI	48.7±12.9	46.8±12.3	47.5±12.5	50.6±13.1	48.4±13.0	52.2±12.7	0.314	-
SRS-22								
activity	2.6±0.5	2.6±0.6	2.6±0.6	2.4±0.6	2.5±0.6	2.2±0.5	0.475	C1 vs. C2*
pain	2.3±0.5	2.2±0.6	2.2±0.5	2.3±0.6	2.2±0.9	1.9±0.8	0.372	C1 vs. C2**
appearance	2.5±0.4	2.6±0.5	2.5±0.4	2.7±0.5	2.4±0.4	2.5±0.5	0.821	-
mental	2.9±0.5	2.8±0.5	2.9±0.5	2.8±0.6	2.8±0.5	2.8±0.5	0.819	-

VAS, visual analogue scale; ODI, Oswestry Disability Index; SRS, Scoliosis Research Society

** indicates p value <0.01; * indicates p value <0.05.

Figures

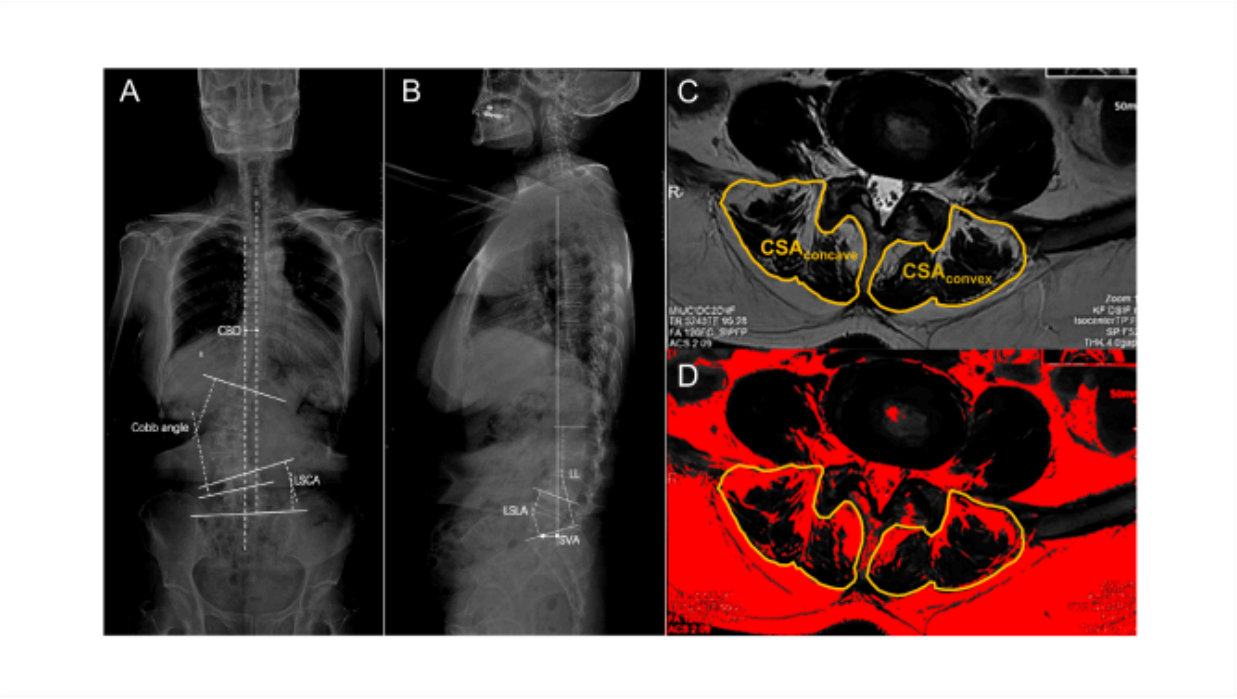


Figure 1

Schematic diagram of (A) coronal parameters on P/A radiograph; (B) sagittal spinal parameters on lateral radiographs; and paraspinal muscle measurements, including: (C) cross-sectional area and; (D) fatty infiltration of bilateral sides.

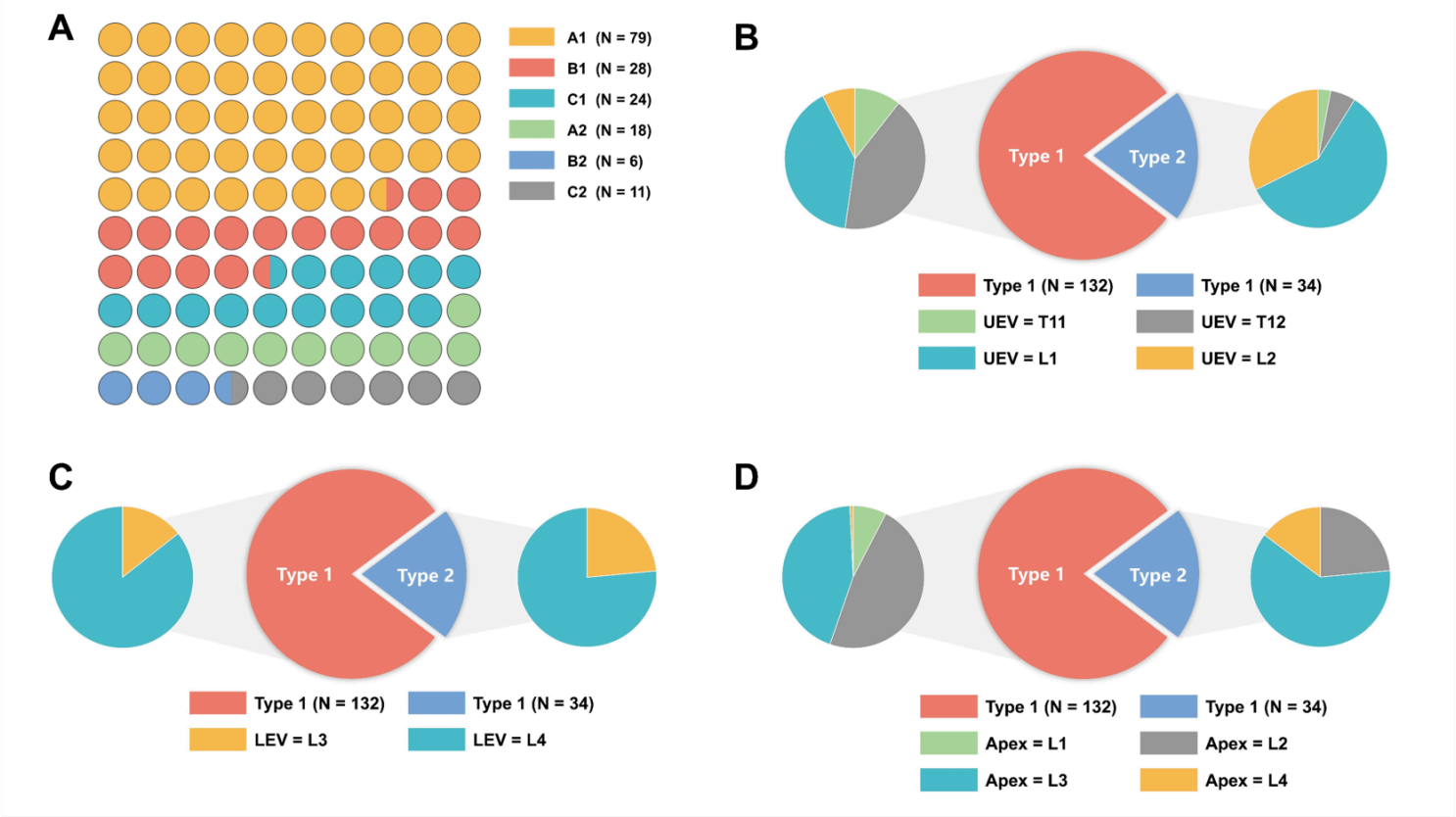


Figure 2

Schematic diagram of subgroup distribution and curve characteristics. Patient subgrouping according to coronal balance distance and pelvic obliquity(A); upper end vertebrae distribution among subgroups (B); lower end vertebrae distribution among subgroups (C); and apex vertebrae distribution among subgroups (D).

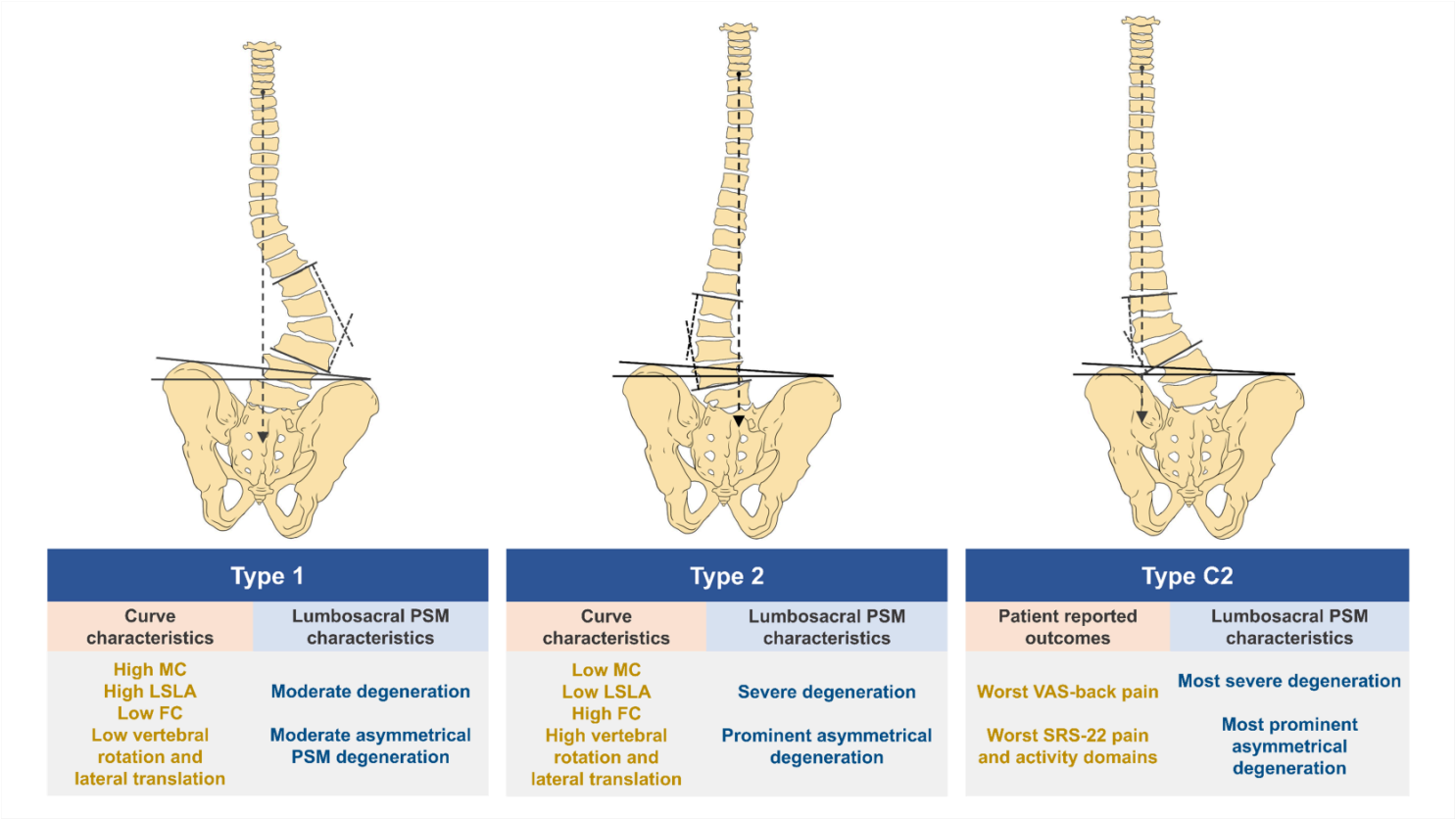


Figure 3

Illustration depicting the spinal coronal alignment characteristics of the 3 groups.